

Dielectric anomalies and spiral magnetic order in CoCr_2O_4

G. Lawes¹, B. Melot², K. Page,² C. Ederer,² M. A. Hayward,³ Th. Proffen⁴ and R. Seshadri²

¹ *Department of Physics and Astronomy,*

Wayne State University, Detroit, MI 48201

² *Materials Department and Materials Research Laboratory*

University of California, Santa Barbara, CA 93106

³ *Department of Chemistry, Inorganic Chemistry Laboratory,*

University of Oxford, South Parks Road, Oxford, OX1 3QR UK and

⁴ *Los Alamos National Laboratory, Manuel Lujan Jr. Neutron Scattering Center*

LANSCE-12, MS H805, Los Alamos, NM 87545

(Dated: June 4, 2018)

Abstract

We have investigated the structural, magnetic, thermodynamic, and dielectric properties of polycrystalline CoCr_2O_4 , an insulating spinel exhibiting both ferrimagnetic and spiral magnetic structures. Below $T_c = 94\text{ K}$ the sample develops long-range ferrimagnetic order, and we attribute a sharp phase transition at $T_N \approx 25\text{ K}$ with the onset of long-range spiral magnetic order. Neutron measurements confirm that while the structure remains cubic at 80 K and at 11 K ; there is complex magnetic ordering by 11 K . Density functional theory supports the view of a ferrimagnetic semiconductor with magnetic interactions consistent with non-collinear ordering. Capacitance measurements on CoCr_2O_4 show a sharp decrease in the dielectric constant at T_N , but also an anomaly showing thermal hysteresis falling between approximately $T = 50\text{ K}$ and $T = 57\text{ K}$. We tentatively attribute the appearance of this higher temperature dielectric anomaly to the development of *short-range* spiral magnetic order, and discuss these results in the context of utilizing dielectric spectroscopy to investigate non-collinear short-range magnetic structures.

PACS numbers: 75.50.Gg, 75.80.+q, 75.40.Cx

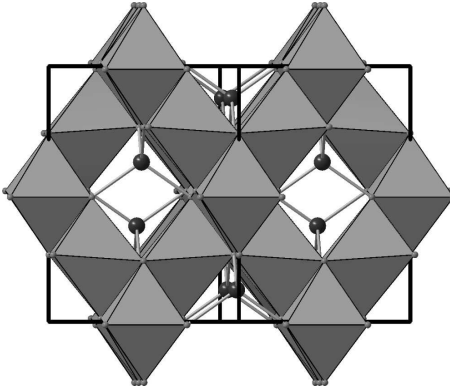


FIG. 1: Structure projected down [110] showing octahedra around Cr and tetrahedral Co atoms.

I. INTRODUCTION

In recent years there has been renewed interest in investigating systems in which charge and spin degrees of freedom are strongly coupled. From colossal magnetoresistive materials¹ to diluted magnetic semiconductors², studies on systems exhibiting an interplay between their magnetic and electronic properties have led to a deeper appreciation of the role of spin-charge coupling in determining the behavior of materials. The long-standing problem of understanding magnetodielectric coupling in insulating magnetic compounds has also been re-visited lately. Recent results on magnetodielectrics have highlighted several important features in these systems, including the observation that incommensurate non-collinear magnetic structures tend to lead to large magnetocapacitive couplings,^{3,4} as does geometrical magnetic frustration. With this background, it is natural to ask how one can use dielectric measurements to extract information about incommensurate non-collinear magnetic structures in frustrated magnets.

CoCr_2O_4 is a spinel ferrimagnet, with Co^{2+} ions on the A sites and Cr^{3+} on the B sites of the spinel structure (FIG. 1). Both Co^{2+} and Cr^{3+} are magnetic; in conjunction with the fact that coupling between the B sites is also quite strong, a complex magnetic phase diagram emerges. Below approximately $T_c = 94\text{ K}$ the system has long-range ferrimagnetic order. There remain some discrepancies concerning the low temperature magnetic phase diagram. In the original investigation on powder CoCr_2O_4 samples, Menyuk *et al.* found evidence for short-range spiral magnetic order below $T \sim 86\text{ K}$, and long-range spiral magnetic order below $T \sim 31\text{ K}$.¹² Motivated by suggestions that ferrimagnetic spiral long-range order in

CoCr_2O_4 should be unstable, Tomiyasu *et al.* investigated both CoCr_2O_4 , and MnCr_2O_4 through extensive neutron and magnetization measurements on single crystals. These more recent studies suggest that the spiral component develops incommensurate short-range order below approximately $T = 50\text{ K}$, and that this short-range order persists to the lowest temperatures with a correlation length of only 3.1 nm at $T = 8\text{ K}$. The authors attribute this behavior to weak geometric magnetic frustration.

These properties suggest that CoCr_2O_4 would be a promising material for investigations on magnetodielectric coupling in systems with non-collinear magnetic order. CoCr_2O_4 is insulating, and has two different types of magnetic structures (ferrimagnetic and spiral). Measuring the dielectric constant in phases with both the ferrimagnetic and spiral components will offer insight into how dielectric properties couple to different magnetic structures within the same material.

II. EXPERIMENTAL AND COMPUTATIONAL DETAILS

Ceramic samples (beautiful jade-green pellets) were prepared from cobalt oxalate $[\text{Co}(\text{C}_2\text{O}_4)_2 \cdot 2\text{H}_2\text{O}]$ and chromium oxide (Cr_2O_3) by heating well-ground mixtures initially at 800°C for close to 24 h followed by regrinding, pelletizing and heating at 1000°C for 24 h. The samples were initially characterized by lab powder x-ray diffraction (Scintag X-II, $\text{CuK}\alpha$ radiation) and then by time-of-flight powder neutron diffraction at room temperatures, 80 K and 11 K at the neutron powder diffractometer (NPDF)⁶ at the Lujan Center at Los Alamos National Laboratory. For the measurements, the samples were contained in vanadium cans.

Calculations were performed using the projector augmented wave⁷ method implemented in the Vienna Ab-initio Simulation Package (VASP).⁸ The cubic spinel structure (space group $Fd\bar{3}m$) with the lattice parameters fixed to the experimentally obtained $a = 8.3351\text{ \AA}$ was used, with an internal structural parameter for the oxygen of $x = 0.264$ determined from the diffraction data. Different collinear magnetic structures were calculated in order to extract the Heisenberg exchange constants. The plane wave energy cut-off was 400 eV and we used a $8 \times 8 \times 8$ Monkhorst-Pack mesh of k -points. The LDA + U method of Dudarev *et al.*⁹ was used and U_{eff} was varied independently on both the Co and Cr sites.

III. RESULTS AND DISCUSSION

We measured the temperature and field dependence of the DC magnetization of CoCr_2O_4 using a Quantum Design MPMS SQUID magnetometer, operating between $T = 5\text{ K}$ and $T = 350\text{ K}$, and measured the AC magnetization of the sample on a Quantum Design Physical Property Measurement System PPMS at frequencies between $\omega/2\pi = 100\text{ Hz}$ and $\omega/2\pi = 10\text{ kHz}$. We measured the specific heat of CoCr_2O_4 as a function of temperature and magnetic field with a quasi-adiabatic method on the PPMS using a 20 mg pressed powder pellet. We found that the internal time constant of the sample was significantly smaller than the other time constants in the fit, suggesting excellent thermal coupling between the sample and calorimeter. In order to measure the dielectric constant, we pressed approximately 75 mg of CoCr_2O_4 into a $5\text{ mm} \times 5\text{ mm} \times 1.5\text{ mm}$ pellet, and fashioned electrodes on opposite faces of the pellet using conducting silver epoxy. We measured the dielectric constant between $\omega/2\pi = 1\text{ kHz}$ and $\omega/2\pi = 1\text{ MHz}$ with an Agilent 4284A LCR meter, using the PPMS for temperature and magnetic field control. The data at lower frequencies was qualitatively similar to the higher frequency measurements, although they were somewhat noisier and displayed larger losses, possibly due to conduction at the grain boundaries.

Figure 2 shows the magnetization as a function of temperature measured on warming after cooling in a magnetic field (upper panel). These data are qualitatively similar to the FC data obtained by Tomiyasu *et al.*⁵ The magnetization shows a large increase below the onset of ferrimagnetic long range order at $T_c = 95\text{ K}$, and there is an anomaly at $T_S = 27\text{ K}$ associated with spiral magnetic order in the system. It should be noted that the anomaly at $T_S = 27\text{ K}$ is sharper than that presented in the Tomiyasu *et al.* data.⁵

The lower panel of Fig. 2 plots the AC magnetization measurements at 10 kHz. The real part of the susceptibility exhibit a very large peak at T_c . The inset to the lower panel of Fig 2 shows the low temperature AC susceptibility in more detail. There is a very clear peak in χ' at $T_S = 27\text{ K}$, consistent with the sharp anomaly in the DC magnetization measurements. Furthermore, there is another clear magnetic feature at approximately $T = 13\text{ K}$, which is rather more difficult to observe in the DC measurements. Tomiyasu *et al* associate this feature with a saturation of the correlation length for the spiral component on cooling.⁵ These bulk magnetization measurements conclusively show the existence of magnetic features at $T_c = 95\text{ K}$ and $T_S = 27\text{ K}$, associated with the ferrimagnetic and spiral magnetic structures

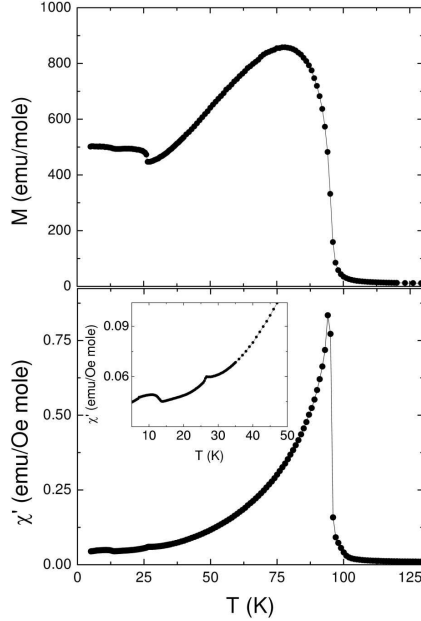


FIG. 2: Upper panel: Field-cooled DC magnetization of CoCr_2O_4 measured in an applied field of $H=100$ Oe. Lower Panel: Real part of the AC susceptibility of CoCr_2O_4 measured at $H=0$ and $\omega/2\pi=10$ kHz. Inset: Lower temperature magnetic anomalies in CoCr_2O_4 .

respectively, and a third magnetic feature at $T = 13$ K.

In order to get more information about the magnetic transitions in CoCr_2O_4 , we also conducted neutron measurements on these samples. Figure 3 displays the results of fitting the low-angle time-of-flight neutron diffraction data from CoCr_2O_4 powders to the *nuclear* structure. At room temperature, the data is almost completely fit except for a small reflection near $d = 2.15$ Å which corresponds to the sample container. At 80 K, below the first collinear magnetic ordering temperature, we find that some of the peaks whose nuclear contribution is fit, have a residual intensity seen clearly in the difference spectra, particularly near $d = 1.7$ Å and 1.9 Å, due to magnetic ordering. At 11 K, the data reveal a number of peaks whose intensities are not correctly fit, as well as new reflections which have come about because of the long-range non-collinear magnetic order, again evident in the difference spectrum. In particular, the low-angle peak at 2.7 Å is evident only in the 11 K data as are peaks near $d = 1.7$ Å and $d = 2.2$ Å. While we have not at this stage been able to completely establish the magnetic structure, we present these data to strengthen our interpretation of the magnetic and transport measurements.

The electronic structure of CoCr_2O_4 was calculated using the LSDA + U methodology.

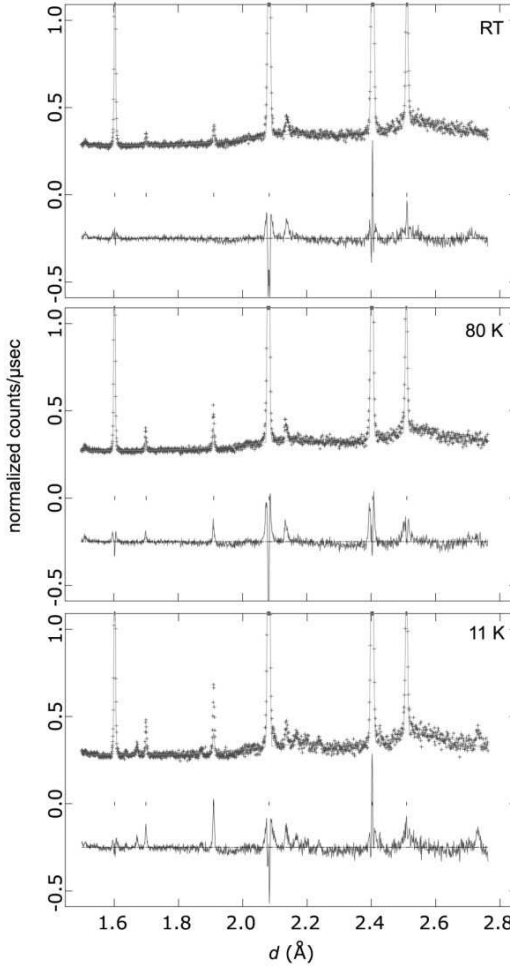


FIG. 3: Time-of-flight neutron powder diffraction at room temperature, 80 K and 11 K. The symbols in each panel are data, the lines are fits using the Rietveld method to the nuclear structure, and the traces at the bottom of each panel are the difference profiles. The peaks in the difference profiles that emerge as the temperature is lowered arise from long-range magnetic ordering.

FIG. 4 displays the total density of states (DOS) and the partial densities of Co d and Cr d states obtained using $U_{\text{eff}}^{\text{Co}} = U_{\text{eff}}^{\text{Cr}} = 0$ eV (LSDA, top panel), as well as $U_{\text{eff}}^{\text{Co}} = 4$ eV and $U_{\text{eff}}^{\text{Cr}} = 2$ eV (lower panel) and a collinear Néel-type magnetic structure (Co spins antiparallel to Cr spins). The system is an insulating fully spin-polarized ferrimagnetic semiconductor already in LSDA, albeit with a very small gap, less than 0.1 eV. Application of U on either of the two magnetic sites enlarges the gap but only application of U on both sites leads to a significant gap of > 1 eV. The calculations show that this system can be expected to be a robust insulator and therefore promising for magnetodielectric measurements.

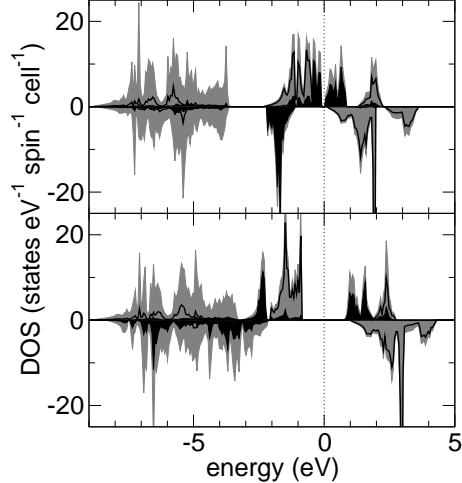


FIG. 4: Total densities of state (gray shaded) and partial densities of Co d (black shaded) and Cr d (black line) states obtained for $U_{\text{eff}}^{\text{Co}} = U_{\text{eff}}^{\text{Cr}} = 0$ eV (LSDA, top panel), as well as $U_{\text{eff}}^{\text{Co}} = 4$ eV and $U_{\text{eff}}^{\text{Cr}} = 2$ eV (lower panel) and a collinear Néel-type ordering.

We also extracted the Heisenberg exchange coupling constants by calculating the total energy differences for different collinear magnetic configurations. It has been shown by Kaplan¹⁰ that using a simple Heisenberg model for the cubic spinel structure with only nearest neighbor couplings J_{AB} and J_{BB} , the magnetic ground state structure is determined by the parameter $u = (4J_{BB}S_B)/(3J_{AB}S_A)$, where S_A and S_B denote the spins of the A and B -site cations respectively. The collinear ferrimagnetic Néel state is the stable ground state for $u < u_0 = 8/9$, whereas for larger values of u non-collinear spiral ordering is expected. The Heisenberg exchange constants extracted from our calculations, using the reasonable values $U_{\text{eff}}^{\text{Co}} = 4$ eV and $U_{\text{eff}}^{\text{Cr}} = 2$ eV, are: $S_A J_{AB} S_B = 5.0$ meV, $S_B J_{BB} S_B = 2.4$ meV, and $u = 0.65$. Increasing $U_{\text{eff}}^{\text{Co}}$ and decreasing $U_{\text{eff}}^{\text{Cr}}$ leads to a larger value of u , eventually exceeding the critical value $u_0 = 8/9$. In addition, we also extracted the coupling constant J_{AA} which is neglected in the treatment of Kaplan. For the same values of U as above ($U_{\text{eff}}^{\text{Co}} = 4$ eV and $U_{\text{eff}}^{\text{Cr}} = 2$ eV) we obtain $S_A J_{AA} S_A = 0.7$ meV. This value is not necessarily negligible and indicates that the coupling between the A-site cations could play an important role in the magnetic properties of cubic spinels and in fact lead to non-collinear magnetic order even for values of u smaller than $u_0 = 8/9$. The possible importance of A-site coupling has also been pointed out in a recent experimental study of the spinel systems $M\text{Al}_2\text{O}_4$ ($M=\text{Co, Fe, Mn}$)¹¹. A detailed analysis of the U dependence of the electronic structure and

magnetic couplings in CoCr_2O_4 is in progress. From the preliminary results presented in this work it can be concluded that the calculated values of the exchange coupling constants are consistent with the appearance of non-collinear magnetic order and that A site coupling might be important to understand the magnetic properties of this system.

In an attempt to establish whether the spiral magnetic transition at $T_S = 27\text{ K}$ is long range¹² or short range⁵, we measured the specific heat of our polycrystalline CoCr_2O_4 sample. The thermodynamic data presented in FIG. 5, including both the lattice and magnetic contributions to heat capacity, strongly suggests that there are two transitions to magnetic states with long range order, one occurring with $T_c = 94\text{ K}$ and the second at $T_S = 27\text{ K}$. Specifically, the sharp peak in C/T at $T_S = 27\text{ K}$ is indicative of long range collective ordering. We can calculate the entropy under the peaks in the upper panel of FIG. 5 to estimate the fraction of spins participating in the long range order at each transition. The entropy lost by CoCr_2O_4 at T_c is approximately 0.1 J/K per mole, while the entropy change at $T_S = 27\text{ K}$ is approximately 0.15 J/K per mole, both at $H = 0$. These changes in entropy are small compared to the expected change in entropy for fully spin ordered CoCr_2O_4 of 34.6 J/K per mole (using the spin-only values for Co^{2+} and Cr^{3+}). This is consistent with the relatively large specific heat exhibited by CoCr_2O_4 over the entire temperature range shown, which suggests that significant short range magnetic order is likely developing over a wide range of temperatures. We do not see any features in specific heat which could be associated with a thermodynamic transition occurring at $T = 13\text{ K}$; this low temperature anomaly in the magnetization does not involve any measurable change in entropy of the system.

The lower panel of FIG. 5 plots the dependence of the $T_S = 27\text{ K}$ transition at two different magnetic fields. The $H = 0$ peak appears to be somewhat larger than that plotted in the upper panel. This is because the higher density of data points more accurately captures the proper shape of the peak. The amount of entropy under the peak is practically unchanged. The transition temperature is almost completely independent of applied magnetic field, but the magnitude of the peak is suppressed by over a factor of two at $H = 5\text{ T}$ as compared to the zero field data. This suggests that fewer spins undergo long-range spiral order at $T_S = 27\text{ K}$ at larger magnetic fields, but it is impossible to tell from the data if the extra entropy is removed at higher or lower temperatures.

One of the primary motivations for these experiments was to investigate what effect the ferrimagnetic and spiral magnetic transitions would have on the dielectric constant of

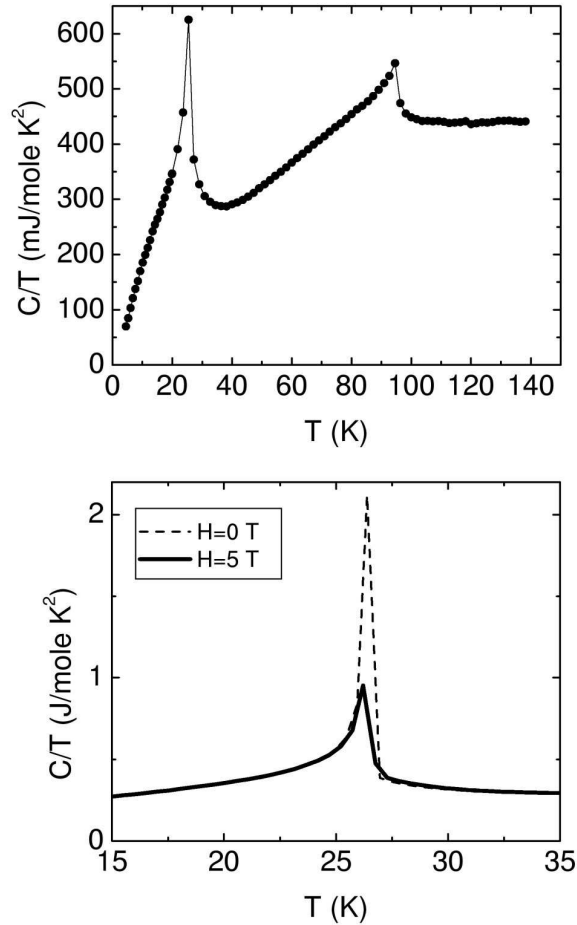


FIG. 5: Upper Panel: Specific heat measurements on CoCr_2O_4 plotted as C/T vs T . Lower Panel: Specific heat of CoCr_2O_4 at the $T_S = 27\text{ K}$ transition, measured at $H = 0\text{ T}$ and $H = 5\text{ T}$.

CoCr_2O_4 . These data are plotted in the upper and middle panels FIG. 6, which shows the dependence of the dielectric constant on temperature for two different polycrystalline CoCr_2O_4 samples measured on warming. In both these samples, the dielectric constant depends only weakly on temperature, with sample B showing a variation of approximately 1% over the entire temperature range, and sample A showing an even smaller change. Differences in the magnitude of the dielectric constant can be attributed to errors in determining the geometrical capacitance factor. Differences in the temperature dependence may possibly arise from small differences in conductivity between the two samples. Preliminary measurements suggest that sample B is slightly more conducting than sample A, although this needs to be investigated in more detail. Both samples were structurally identical (verified by powder x-ray diffraction) but sample B was better sintered.

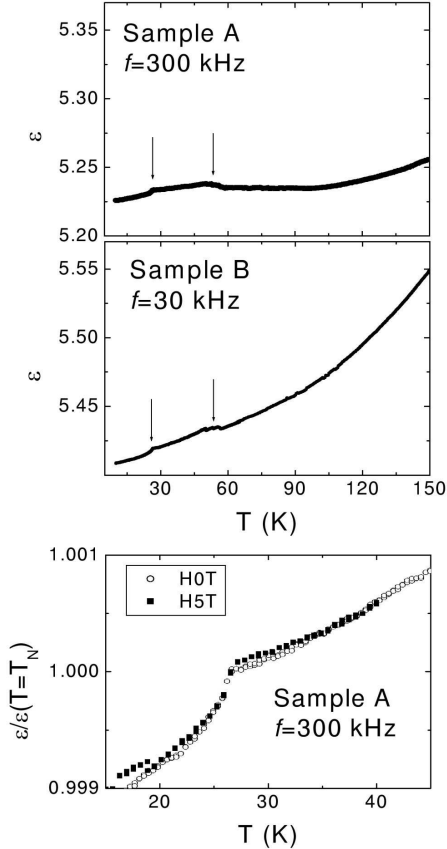


FIG. 6: Top Panel: Dielectric constant of CoCr_2O_4 sample A measured at $H=0$ as a function of temperature measured at $\omega/2\pi=300$ kHz. Middle Panel: Dielectric constant of CoCr_2O_4 sample B measured at $H=0$ as a function of temperature measured at $\omega/2\pi=30$ kHz. The arrows indicate the location of the observed dielectric anomalies. Bottom Panel: Relative dielectric constant of CoCr_2O_4 sample A at the spiral ordering transition at $H=0$ and at $H=5$ T.

The general features in the dielectric constant are very similar for both these samples. Most notably, there is a well-defined drop in dielectric constant coincident with the onset of long range spiral magnetic order at $T_S = 27$ K (indicated with an arrow). This sharp decrease is a signature of the coupling between the dielectric properties and magnetic structure. The change in dielectric constant is fairly small, only 0.2% between $T_S = 27$ K and the base temperature. This should be compared with EuTiO_3^{13} and SeCuO_3^{14} which show larger changes on ordering (3.5% and 2% respectively). The small magnitude of the shift in the dielectric constant CoCr_2O_4 at the spiral ordering transition may result from the fact that only a small fraction of spins order at this temperature, as evidenced by the

thermodynamic data discussed previously. This dielectric anomaly is almost completely independent of magnetic field as well (lower panel of FIG. 6). An applied magnetic field of $H = 5$ T introduces almost no shift in either the temperature or magnitude of the anomaly. A magnetic field does however introduce a small shift in the overall dielectric constant, on the order of 0.01% in a field of $H = 1$ T (not shown).

There is no clear dielectric feature at the ferrimagnetic ordering temperature T_c . There may be a subtle change of slope observable in Sample A, but this is not seen in Sample B, which shows much larger intrinsic dependence of dielectric constant on temperature. The lack of a sharp anomaly at T_c suggests that there is only weak coupling between the dielectric constant of CoCr_2O_4 and the ferrimagnetic component of the magnetic structure. Furthermore, there is no dielectric feature associated with the $T = 13$ K transition. Since this magnetic feature is believed to be related to the spiral magnetization component⁵, one would expect to see a clear anomaly at 13 K. However, specific heat measurements show that only a small number of spins are likely to be involved in this transition, which perhaps explains the absence of any dielectric feature.

The dielectric constant of CoCr_2O_4 couples only to the spiral spin structure, and not to the ferrimagnetic structure. The shift in dielectric constant observed in many magnetodielectric materials is believed to arise from strong spin-phonon coupling^{13,14}. Within this framework, the phonon mode giving rise to this magnetodielectric behavior must not couple to magnetic order along the (001) direction, but should be sensitive to spiral spin-ordering with a propagation vector along the $Q=(\delta, \delta, 0)$ direction in the (001) plane⁵. This observation provides an important symmetry restriction on allowed forms for the spin-lattice coupling in CoCr_2O_4 . Further investigations on the microscopic mechanisms for spin-phonon coupling in CoCr_2O_4 will rely on a detailed understanding of the phonon modes in this system.

We find evidence for one further temperature dependent dielectric anomaly in CoCr_2O_4 . The dielectric constant shows a distinct peak at approximately $T = 50$ K for the two samples (indicated by arrows in FIG. 6). More precisely, measurements on Sample B seem to indicate the presence of a series of peaks, while Sample A rather exhibits one broader peak. The magnitude of the increase in dielectric constant at this temperature is comparable to the decrease in dielectric constant below $T_S = 27$ K. However, the origins of this feature are less clear. Neither the magnetization data in FIG. 2 nor the specific heat data in FIG. 6

show any evidence for a phase transition at this temperature. Additionally, this anomaly has a rather broad onset, which varies somewhat with sample history. Since CoCr_2O_4 does not have any structural phase transitions at low temperatures, this anomaly must have a magnetic origin. Specifically, we believe that this dielectric anomaly arises from the onset of short range spiral magnetic order, which has also been shown to occur at approximately $T = 50 \text{ K}$ ⁵.

As a further probe of this anomaly, we measured the dielectric constant on warming and cooling at different rates. FIG. 7 plots the dielectric constant of CoCr_2O_4 measuring on warming and cooling at 1 K/min. (upper panel) and 5 K/min. (lower panel). In both cases, there is *no* anomaly when the dielectric constant is measured on cooling, but there is a clear feature in the dielectric constant when the sample is warmed. Furthermore, the peak temperature for this anomaly occurs at a higher temperature ($T = 50 \text{ K}$) when the sample is warmed at 5 K/min. as compared to when it is warmed at 1 K/min. ($T = 48 \text{ K}$). This thermal hysteresis may arise from a non-equilibrium distribution of regions of short range spiral magnetic order. Below $T_S = 27 \text{ K}$, the thermodynamic and dielectric data suggest that CoCr_2O_4 develops long range spiral order. On warming, the disappearance of a non-equilibrium distribution of short range spiral magnetic clusters may be responsible for the dielectric signal at $T = 50 \text{ K}$. The shift of this anomaly to lower temperatures as the sample is warmed more slowly supports this idea. Conversely, when the sample is cooled from higher temperatures, there would be no spiral magnetic clusters present, and therefore no shift in the dielectric constant.

In summary, we have presented extensive magnetic, thermodynamic, neutron, and dielectric data on CoCr_2O_4 . These results are consistent with a phase transition to a ferrimagnetically ordered state at $T=94 \text{ K}$ and we have conclusive evidence for a second transition to a phase with long-range spiral magnetic order below $T_S = 27 \text{ K}$ in our polycrystalline sample. Magnetocapacitive measurements show that the dielectric constant of CoCr_2O_4 couples strongly to the spiral magnetic order parameter, but is insensitive to the ferrimagnetic spin component. This limits the allowed spin-phonon coupling symmetry in this system, and places restrictions on the possible microscopic mechanism for the observed magnetodielectric shifts. The dielectric constant of CoCr_2O_4 is also found to be affected by the development of short-range spiral magnetic order. This suggests that in materials with strong spin-phonon coupling, it may be possible to use capacitive measurements to probe short-range magnetic

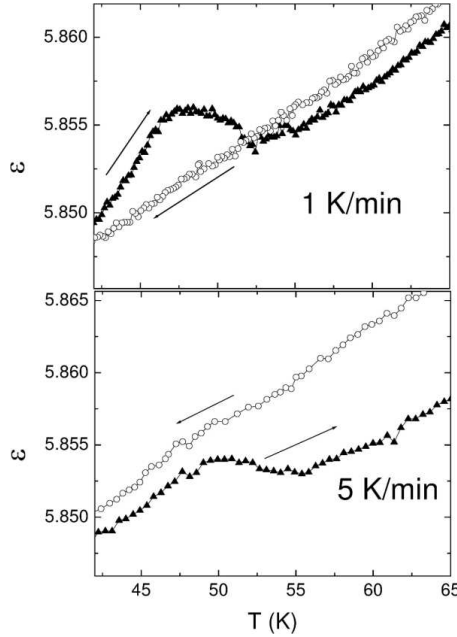


FIG. 7: Upper Panel: Dielectric constant of CoCr_2O_4 near $T=50$ K measured on cooling and warming at 1 K/min. Lower Panel: Dielectric constant of CoCr_2O_4 near $T=50$ K measured on cooling and warming at 5 K/min. In both plots, the arrows indicate the temperature change.

correlations.

Acknowledgements

This work in UCSB was supported by National Science Foundation through the MRL program (DMR00-80034), through a Chemical Bonding Center (CHE04-34567). Measurements at the Lujan Center at Los Alamos Neutron Science Center were supported by the Department of Energy Office of Basic Energy Sciences and Los Alamos National Laboratory funded by Department of Energy under contract W-7405-ENG-36. MAH thanks the Royal Society for funding.

¹ S. Jin, T.H. Tiefel, M. McCormack, R.A. Fastnacht, R. Ramesh, L.H. Chen, *Science* **264**, 413 (1994).

² H. Ohno, *Science* **281**, 951 (1998).

³ T. Goto, T. Kimura, G. Lawes, A.P. Ramirez, and Y. Tokura, *Phys. Rev. Lett.* **92**, 257201 (2004).

⁴ T. Kimura *et al.*, *Nature* **425**, 55 (2003).

⁵ K. Tomiyasu, J. Fukunaga, and H. Suzuki, *Phys. Rev. B* **70**, 214434 (2004).

⁶ Th. Proffen, T. Egami, S.J.L. Billinge, A.K. Cheetham, D. Louca, and J.B. Parise, *Appl. Phys. A* **74**, 163 (2002).

⁷ P. E. Blöchl, *Phys. Rev. B* **50**, 17953 (1994).

⁸ Vienna Ab-Initio Simulation Package, <http://cms.mpi.univie.ac.at/vasp/vasp/vasp.html>

⁹ S. L. Dudarev, G. A. Botton, S. A. Savrasov, Z. Szotek, W. M. Temmerman and A. P. Sutton, *Phys. Status Solidi A* **166**, 429 1998.

¹⁰ T. A. Kaplan, *Phys Rev.* **119**, 1460 (1960).

¹¹ N. Tristan, J. Hemberger, A. Krimmel, H.-A. Krug von Nida, V. Tsurkan, and A. Loidl, *Phys. Rev. B* **72**, 174404 (2005).

¹² N. Menyuk, K. Dwight, and A. Wold, *J. Phys. (Paris)* **25**, 528 (1964).

¹³ T. Katsufuji and H. Takagi, *Phys. Rev. B* **64**, 054415 (2001).

¹⁴ G. Lawes, A.P. Ramirez, C.M. Varma, and M.A. Subramanian, *Phys. Rev. Lett.* **91**, 257208 (2003).